Received: 25 September 2023 | Revised: 13 November 2023 | Accepted: 15 November 2023

DOI: 10.1002/pol.20230724

RESEARCH ARTICLE

JOURNAL OF POLYMER SCIENCE WILEY

One-pot method for upcycling polycarbonate waste to yield high-strength, BPA-free composites

Katelyn M. Derr | **Rhett C. Smith**

Department of Chemistry, Clemson University, Clemson, South Carolina, USA

Correspondence
Rhett C. Smith, Department of Chemistry, Clemson University, Clemson, SC, 29634, USA.
Email: rhett@clemson.edu

Funding information
Division of Chemistry, Grant/Award Number: CHE-2203669

Abstract

Environmental damage caused by waste plastics and downstream chemical breakdown products is a modern crisis. Endocrine-disrupting bisphenol A (BPA), found in breakdown products of poly(bisphenol A carbonate) (PC), is an especially pernicious example that interferes with the reproduction and development of a wide range of organisms, including humans. Herein we report a single-stage thiocracking method to chemically upcycle polycarbonate using elemental sulfur, a waste product of fossil fuel refining. Importantly, this method disintegrates bisphenol A units into monoaryls, thus eliminating endocrine-disrupting BPA from the material and from any potential downstream waste. Thiocracking of PC (10 wt%) with elemental sulfur (90 wt%) at 320 °C yields the highly crosslinked network **SPC$_{90}$**. The composition, thermal, morphological, and mechanical properties of **SPC$_{90}$** were characterized by FT-IR spectroscopy, TGA, DSC, elemental analysis, SEM/EDX, compressive strength tests, and flexural strength tests. The composite **SPC$_{90}$** (compressive strength = 12.8 MPa, flexural strength = 4.33 MPa) showed mechanical strengths exceeding those of commercial bricks and competitive with those of mineral cements. The approach discussed herein represents a method to chemically upcycle polycarbonate while deconstructing BPA units, and valorizing waste sulfur to yield structurally viable building materials that could replace less-green legacy materials.

KEYWORDS

bisphenol A, composites, polycarbonate, recycling, sulfur, thiocracking, upcycling

1 | INTRODUCTION

Poly(bisphenol A carbonate) (PC) is used for many applications due to its impact resistance, thermal stability, and optical properties.[1–3] Although significant developments have been reported in chemical[4–8] and physical recycling[9,10] methods for PC, most post-consumer polycarbonate is landfilled. Landfilled PC is particularly detrimental because one of its environmental breakdown products is bisphenol A (BPA). BPA can easily leach into soil and water, where it acts as an endocrine disruptor by binding estrogen receptors in living organisms, leading to a panoply of issues such as low birth weights, premature delivery, and miscarriage.[11]

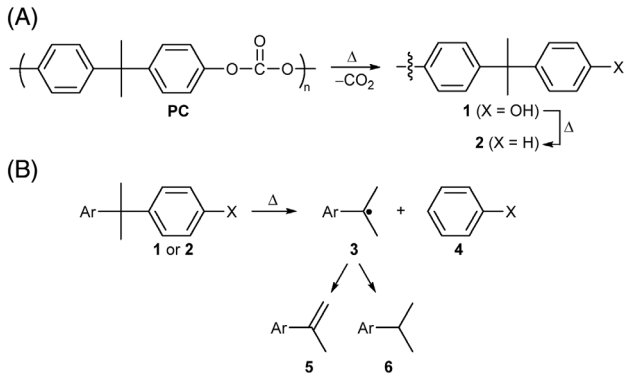

SCHEME 1 Known routes for the thermal decomposition of poly(bisphenol A carbonate) polymer backbone (A) and of resultant BPA fragments (B) relavant to microstructures observed in the current study.

Chemical recycling approaches for PC have primarily relied on thermal breakdown mechanisms or hydrolysis to give BPA and carbonates. When heated neat under an inert atmosphere at temperatures of 280–340 °C, PC breaks down into molecular fragments including significant quantities of CO and CO_2 within only a few hours.[12–23] Under these conditions the PC backbone decomposes through various pathways (those most relevant to the current study are summarized in Scheme 1).[14] General pathways to PC degradation include carbonate degradation through isomerization, 1,3-shift, and dehydrogenation (the primary route that produces carbon dioxide). Additionally, some BPA units undergo chain scission to yield fragments such as phenol and styrene derivatives. Hydrolysis largely leads to BPA and carbonates. Chemical recycling is an improvement over landfilling, but each mole of PC repeat unit processed still produces up to an equimolar amount of ecologically hazardous BPA. A simple method to upcycle PC with concomitant chemical disintegration of endocrine-disrupting BPA would be a significant advance for waste PC utilization that would preclude downstream escape of BPA into the environment.

Pyrolysis is currently one of the most-used methods to chemically recycle PC. Unfortunately, PC pyrolysis produces ecologically undesirable CO_2 and can require temperatures of up to 900 °C.[6] Many municipalities no longer classify pyrolysis as recycling on the basis of this high energy cost.[24] Hydrolysis is another promising route for chemical recycling of PC, but also produces BPA and CO_2. Alcoholysis and aminolysis methods to chemically recycle PC also yield BPA, along with either carbonates or urea, respectively.[23] A comparably small amount of PC is mechanically recycled for use in less valuable products.[25]

Thiocracking is a recently developed route to plastic recycling/upcycling that involves heating organic substrates with elemental sulfur to facilitate molecular breakdown and conversion of plastic waste to other species.[26] Thiocracking was recently employed as a single-stage process to chemically upcycle poly(ethylene terephthalate) (PET). In this approach, PET, geraniol, and elemental sulfur were heated at 320 °C under an inert atmosphere, leading to tandem transesterification, S—C_{aryl} bond formation, and S—C_{alkyl} formation (inverse/vulcanization), yielding composite **SPG**.[26] **SPG** exhibited an impressive compressive strength of 23.1 MPa, exceeding that required (17 MPa) of ordinary Portland cement (OPC) for residential housing foundations and footings.[27]

We previously carried out mechanistic studies on the reaction of sulfur and *O,O′*-dimethyl bisphenol A under conditions identical to those used in the thiocracking of PET to produce **SPG**.[28] The product of this reaction was a high sulfur-content material (HSM), **BC_{90}**, which exhibited higher compressive strength than OPC. Further analysis revealed that the crosslinked network structure endowing **BC_{90}** with its high mechanical strength features nine unique microstructures resulting from S—C_{aryl} bond-formation and C—C σ-bond scission. Most notably, thiocracking broke down >95% of BPA units to monoaryl species in that study.

Given the effective disintegration of BPA units in the small molecular BPA derivative, we hypothesized that thiocracking could be an effective way to convert polycarbonate into a BPA-free composite that may be a useful structural material. Herein we report a single-stage method to chemically upcycle polycarbonate by thiocracking with 90 wt% elemental sulfur at 320 °C for 2 h. This process yields composite **SPC_{90}**, which displayed compressive strength over double that of commercial brick and approaching that of OPC.

2 | RESULTS AND DISCUSSION

2.1 | Synthesis and chemical/surface characterization of composite SPC_{90}

The polycarbonate-sulfur composite **SPC_{90}** was prepared by heating 10 wt% poly(bisphenol A carbonate) (PC) with 90 wt% elemental sulfur for 2 h at 320 °C in a Parr bomb reactor. During reaction, the pressure of the reactor reached 400 psi. This rise in pressure corresponds to 3.8 mmol of gas evolution, accounting for conversion of at least 77% of carbonate carbons to CO/CO_2(*g*) via mechanisms in Scheme 1. Upon cooling the reaction mixture, **SPC_{90}** was a homogeneous black solid. When remelted, composite **SPC_{90}** formed a highly viscous liquid that could not be readily poured into molds to shape the material. The material was more conveniently fabricated into shapes, such as cylinders for testing compressive

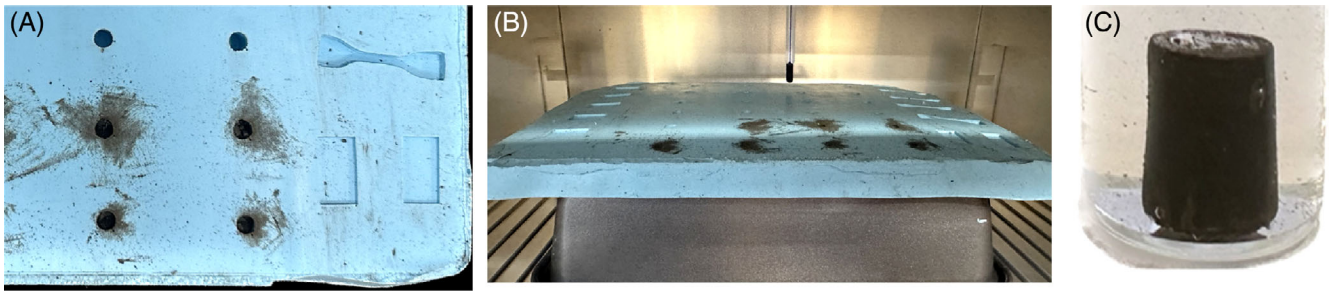

FIGURE 1 Preparation of **SPC_{90}** samples for mechanical strength testing involved placing finely powdered **SPC_{90}** in a silicone mold (A) and then heating the powder in an oven for 2 h at an air temperature of to 160 °C (B) to produce cylindrical samples for compressive testing. Cylinders were used for compressive strength tests and other cylinders were submerged in acidic solution before testing (C).

strength and rectangular prisms for testing flexural strength (Figure 1), by placing a fine powder of **SPC_{90}** into the appropriate silicone mold, followed by curing at 160 °C for 2 h in an oven. The density of **SPC_{90}** fabricated in this way was found to be 1.9 g/cm^3, consistent with other HSMs, and notably lower than grade 53 OPC (3.15 g/cm^3), thus qualifying **SPC_{90}** as a lightweight cement.[29–31]

The sulfur in HSMs like **SPC_{90}** is often incorporated as a mixture of sulfur catenates covalently bound to organic comonomers, and free sulfur species not covalently linked in the network, known as "dark sulfur."[32,33] Dark sulfur can be extracted from composites using toluene, leaving behind only the highly crosslinked, insoluble network containing covalently incorporated sulfur catenates. To quantify the free sulfur in **SPC_{90}**, a finely powdered composite sample was recursively washed with toluene until there was no more extractable mass. After evaporation of the toluene, elemental microanalysis of the soluble fraction of **SPC_{90}** confirmed that extractable mass comprised of 98% sulfur. Nearly all organic material from PC was successfully incorporated into the network and no significant loss of organic material due to extraction was observed. This procedure revealed that 62% of **SPC_{90}** was extractable sulfur. This is comparable to other HSMs prepared from aromatic-containing polymers, such as the aforementioned **SPG** (82% solubilized sulfur).[28]

One of the challenges of characterizing HSMs is that the organic-containing fraction of the composite is insoluble because it is highly crosslinked. Solid state spectroscopic characterization is also hindered because the **SPC_{90}** is 90 wt% sulfur, so the signal from the organic moieties is approximately an order of magnitude weaker than it would be in a structurally analogous pure organic compound. An effective strategy to overcome these drawbacks is to depolymerize the HSM using $LiAlH_4$ or $AlBr_3$.[34,35] Both of these reagents will break the S—S bonds in the sample, but the two depolymerization agents show divergent reactivity with S—C bonds. All of

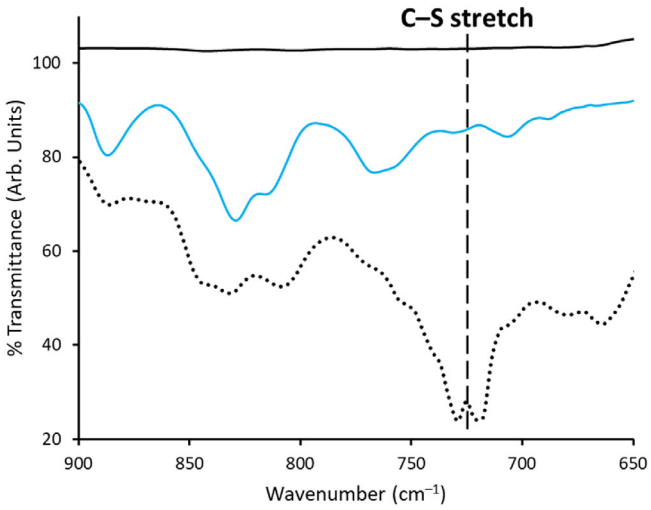

FIGURE 2 FT-IR spectra for **SPC_{90}** (solid black trace), PC (blue trace), and **d-SPC_{90}** (dotted trace) demonstrated the formation of S—C bonds by the emergence of the band centred at 725 cm^{-1}. The full spectra are provided in Figure S1.

the S—C bonds are left intact following treatment with $LiAlH_4$, whereas treatment with $AlBr_3$ leads to breakage of S—C_{alkyl} bonds while S—C_{aryl} bonds are left intact. In the current case, we employed both of these depolymerization strategies to give soluble small molecular organosulfur species able to be characterized by solution spectroscopic techniques. The value of the depolymerization approach is evident from the infrared spectroscopic analysis of PC, **SPC_{90}**, and depolymerized **SPC_{90}** (d-**SPC_{90}**), Figure 2; the sample depolymerized by the action of $AlBr_3$ is shown, and full spectra are provided in Figure S1). As predicted, the IR spectrum of **SPC_{90}**, being 90 wt% sulfur, shows only weak signals for organic species, especially for weak bands such as the S—C stretch. The spectrum for d-**SPC_{90}** provides significantly more insight when compared to the spectrum of PC starting material. Notably, the PC C═O stretch at ~1760 cm^{-1} is absent from the d-**SPC_{90}** spectrum. Likewise, the C—H

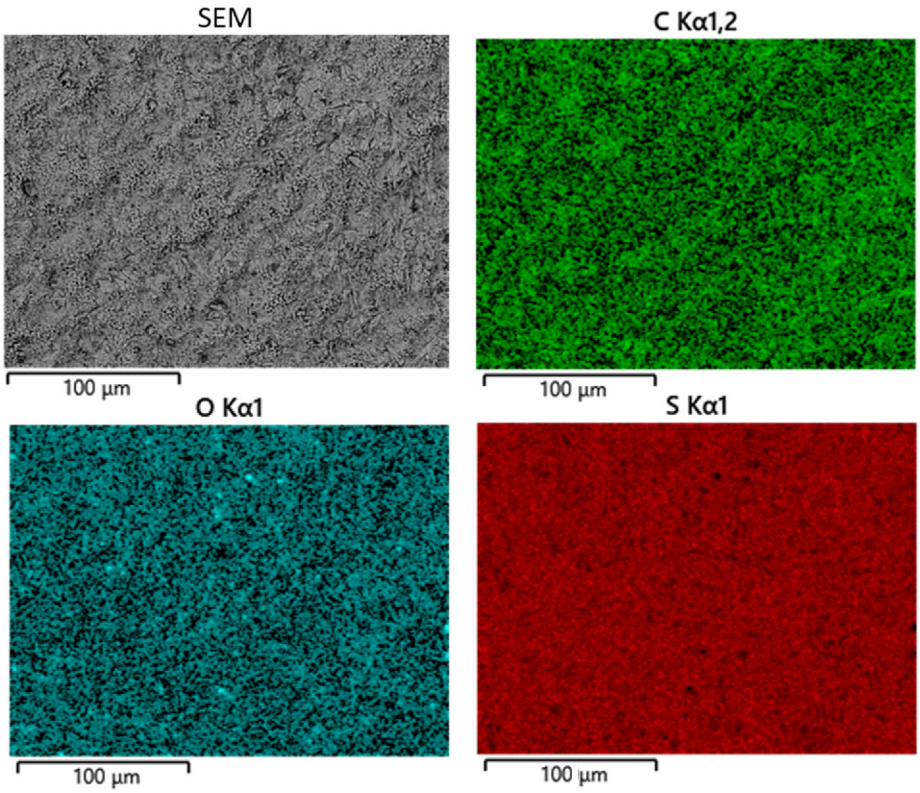

FIGURE 3 Surface analysis of the **SPC$_{90}$** by SEM (gray) with elemental mapping by EDX for carbon (green), oxygen (cyan), and sulfur (red). The scale bar in each image is 100 microns.

stretch ~830 cm^{-1} and C—O stretch (1220–1150 cm^{-1}) have been drastically reduced in intensity when comparing PC to d-**SPC$_{90}$** spectra. There were also apparent C—S stretch frequencies for d-**SPC$_{90}$** at 717 and 729 cm^{-1}, within the range where this band is generally observed in HSMs having S—C$_{aryl}$ bonds.[36]

As shown in Scheme 1, the known thermal breakdown products of PC include species that can engage in S—C$_{benzylic}$ bond-formation (**3** and **6**),[34,37] S—C$_{aryl}$ bond-formation (**4**)[38] and S—C$_{alkyl}$ bond-formation (**5**)[34,39] by established routes. The GC–MS analysis of d-**SPC$_{90}$** showed no intact BPA-containing moieties, regardless of whether $LiAlH_4$ or $AlBr_3$ facilitated depolymerization. The lack of any observable intact BPA moieties from **SPC$_{90}$** is consistent with our previous report on the action of elemental sulfur on model compound *O*,*O*′-dimethyl bisphenol A (DMBPA) under conditions identical to those used to prepare **SPC$_{90}$** from PC. In the case of DMBPA, >95% conversion of BPA to monoaryl derivatives was observed.[28] GC–MS analysis also revealed several monoaryl species having S—C$_{aryl}$ bonds, consistent with prior reports on the reactions of elemental sulfur with phenol derivatives (Figure S2).[35,38] Within the detection limits of GC–MS analysis, these data confirm successful one-pot conversion of PC to a BPA-free composite.

In some previous studies, ineffective mixing of organic comonomers with sulfur resulted in phase separation of organic-rich and sulfur-rich domains in the resulting composites,[40,41] including the polymerization of DMBPA to give **BC$_{90}$** mentioned above.[28] Scanning electron microscopy with elemental mapping by energy dispersive X-ray analysis (SEM–EDX) was used to assess the surface morphology of **SPC$_{90}$** (Figure 3). These images showed that C, O, and S were evenly distributed throughout the material with no evident regions of heterogeneities or phase separation on this scale.

2.2 | Thermal properties of composite SPC$_{90}$

Thermogravimetric analysis (TGA, traces provided in Figure S3) was used to determine the decomposition temperature (T_d, here defined as the temperature at which 5% mass loss occurs upon heating under an atmosphere of $N_2(g)$). Determination of the T_d in HSMs wherein both entrapped orthorhombic sulfur and crosslinked sulfur exist provides insight into the thermal stability of the materials and the contributions of the different components in the material. In **SPC$_{90}$**, for example, a first decomposition temperature occurs at 254 °C due to the sublimation of entrapped *cyclo*-S_8. Other HSMs also exhibit the sublimation of sulfur, though this value is slightly higher than what is usually observed (229 °C for *cyclo*-S_8, for example). A second T_d is observed in **SPC$_{90}$** at 322 °C,

TABLE 1 Thermal and morphological properties of **SPC$_{90}$** with comparison to elemental sulfur.

Materials	T_d[a] (°C)	T_m[b] (°C)	T_g[c] (°C)	Cold crystallization peaks (°C)	ΔH_m (J/g)	ΔH_{cc} (J/g)	Percent crystallinity (χ_c)[d]	Percent insoluble fraction[e]
SPC$_{90}$	219	116	−34	16	27	−15	7	38
S_8	229	118	NA	NA	45	NA	100	0

[a]The temperature at which 5% mass loss was observed.
[b]The temperature at the peak maximum of the endothermic melting.
[c]Glass transition temperature.
[d]The reduction of percent crystallinity of each sample calculated with respect to sulfur (normalized to 100%).
[e]Percent of non-extractable sulfur in each sample after toluene extractions.

attributable to the decomposition/volatilization of the organosulfur domains of the material.

Thermomorphological properties were analyzed using differential scanning calorimetry (DSC), which revealed a glass transition temperature (T_g) of −34 °C (thermograms provided in Figure S4). This T_g is attributable to polymeric sulfur catenates crosslinking the organic moieties. DSC analysis of **SPC$_{90}$** also revealed a cold crystallization peak at 16 °C due to ordering of the sulfur catenates within the material. A melting temperature of 116 °C was also observed, attributable to melting of entrapped *cyclo*-S_8. The relative integrations of melting and crystallization features in the DSC thermograms allow calculation of the enthalpy of melting (ΔH_m) and cold crystallization enthalpy (ΔH_{cc}) for **SPC$_{90}$** (Table 1). These values can be used to calculate the percent crystallinity (χ_c) in **SPC$_{90}$** with respect to sulfur. The percent crystallinity of **SPC$_{90}$** was thus calculated to be 7%, indicating that the material primarily comprises amorphous regions. This is a low percent crystallinity compared to most HSMs comprising 90 wt% sulfur such as **BC$_{90}$** ($\chi_c = 19\%$),[28] **xPES** (made from 90 wt% sulfur and oleyl-esterified PET oligomers, $\chi_c = 25\%$),[42] and **CanBG$_{90}$** (made from canola oil, brown grease, and 90 wt% sulfur, $\chi_c = 12\%$).[30] The low crystallinity in **SPC$_{90}$** is likely attributable to its makeup as a crosslinked network of the several microstructural motifs shown in Figure S2. In contrast, HSMs made exclusively by inverse vulcanization mechanisms can exhibit significant contributions of linear structures that are more prone to forming crystalline domains.[34]

2.3 | Mechanical properties of composite SPC$_{90}$

Cylinders appropriate for compressive strength analysis (Figure 1) were prepared by filling a silicone mold with finely powdered composite and heating the material in the mold in a 160 °C oven for 2 h. Once shaped, the samples were allowed to sit at room temperature in the dark for 96 h before testing, following the procedure used for most other HSMs for which compressive strength data are reported.[26,42–44] The compressive strength of **SPC$_{90}$** was 12.8 ± 1.6 MPa (Table 2; stress–strain plots provided in Figure S5). Whereas **SPC$_{90}$** exhibits a lower compressive strength (12.8 MPa) than **SPG** (23.1 MPa)[26] or **BC$_{90}$** (22.5 MPa),[28] the compressive strength of **SPC$_{90}$** is competitive with common commercial structural materials like bricks (classification C62) used in retaining walls and other non-load bearing applications.[45,46] Several other HSMs comprising 90–95 wt% sulfur exhibit compressive strengths similar to that of **SPC$_{90}$** as well. Examples include **PS$_{95}$** (5% peanut shells, compressive strength = 12.8 MPa),[47,48] **OSS$_{90}$** (10 wt% octenyl succinate-modified corn starch, compressive strength = 10.9 MPa),[49] and **CitS** (10 wt% citronella oil, compressive strength = 10 MPa).[50]

Mineral-based materials, such as brick or ordinary Portland cement (OPC), show significant deterioration under acidic conditions. Conversely, HSMs have demonstrated high resistance to mechanical strength degradation following exposure to acidic environments.[31,43,51,52] To assess whether **SPC$_{90}$** displayed such chemical resistance, cylinders of **SPC$_{90}$** were placed in 0.5 *M* H_2SO_4 for 24 h, conditions under which OPC completely degrades. Following acid exposure, **SPC$_{90}$** retained 76% of its compressive strength (Figure 4 and Table 2; stress–strain plots provided in Figure S5). This strength retention is comparable to that of other HSMs such as terpenoid-sulfur HSMs comprising 90 wt% sulfur, which retain 75%–84% of their compressive strengths after a similar acid challenge.[31,50] The resistance to acid degradation can in part be attributed to the very hydrophobic and nonpolar nature of the HSMs. To further explore the acid-resistance of **SPC$_{90}$** over a longer time span, cylinders were left in the aforementioned acidic conditions for 7 days where they exhibited a compressive strength of 6.3 ± 1.0, retaining 49% of its original strength. In the case of **SPC$_{90}$**, its hydrophobicity and nonporous structure were further validated by water uptake analysis according to conditions ASTM D570, which demonstrated no water uptake within the detection limit, in

TABLE 2 Mechanical properties of **SPC_{90}** compared to other HSMs and commercially available building materials.

Material	Density (g/cm^3)	Compressive strength (MPa)	Flexural strength (MPa)	Compressive strength (% of OPC)
SPC_{90}	1.9	12.8 ± 1.6	3.12 ± 0.53	76
SPG	ND	23.1	4.7	136
BC90	ND	22.5	ND	132
PS_{95}	ND	12.8	5.4	76
OSS_{90}	ND	10.9	5.3	64
CitS	1.8	10	ND	59
C62 Brick	ND	8.6	ND	51
OPC	3.15	17	3.7	100

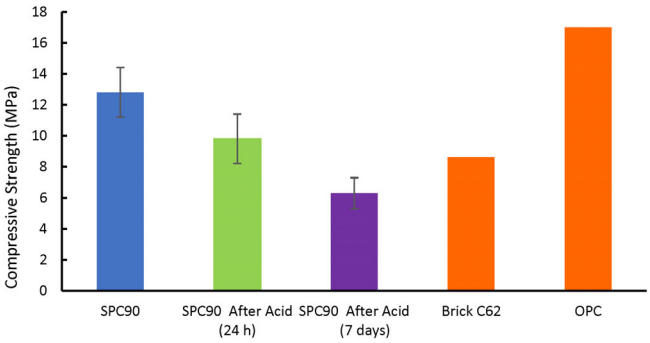

FIGURE 4 Comparison of compressive strength values of **SPC_{90}** cylinders as prepared, after exposure to acid for 24 h, after exposure to acid for 7 days, C62 brick, and OPC.

sharp contrast to mineral cements that often absorb up to 28% of their weight in water.[51]

The flexural strength of **SPC_{90}** was also assessed using rectangular prisms (Figure 1; stress–strain plots provided in Figure S6) clamped in a dynamic mechanical analyzer in single cantilever mode. **SPC_{90}** was found to have a flexural strength of 3.12 ± 0.53 MPa, similar to the range of flexural strengths for OPC and several of the aforementioned HSMs (Table 2).

3 | CONCLUSION

The detrimental effects of BPA-containing polycarbonate degrading in the environment and increasing use of consumer plastics create a pressing need for effective recycling to mitigate environmental damages. This study provides a single-stage process for recycling polycarbonate while repurposing industrial waste sulfur. Thiocracking polycarbonate with elemental sulfur results in a durable material with competitive compressive and flexural strengths while destroying the BPA unit of polycarbonate through thermal degradation. Additional sustainability advantages of **SPC_{90}** over bricks is that **SPC_{90}** solid can be pulverized and reshaped by heating the powder in a mold to 160 °C for only 2 h, whereas bricks require heating to 800–1100 °C for 10–40 h in a kiln for initial shaping and bricks cannot be readily reshaped once they break. Additional studies are underway to assess other characteristics of **SPC_{90}** for long-term durability and viability as diverse components of the build environment.

4 | EXPERIMENTAL SECTION

4.1 | General considerations

Fourier transform infrared spectra were obtained using an IR instrument (Shimadzu IRAffinity-1S) with an ATR attachment. Scans were collected over the range 400–4000 cm^{-1} at ambient temperature with a resolution of 8 cm^{-1}.

TGA data were recorded (Mettler Toledo TGA 2 STARe System) over the range 20–800 °C with a heating rate of 10 °C·min^{-1} under a flow of N_2 (100 mL·min^{-1}). Each measurement was acquired in triplicate, and the presented results represent an average value.

DSC data were acquired (Mettler Toledo DSC 3 STARe System) over the range—60 to 140 °C with a heating rate of 10 °C·min^{-1} under a flow of N_2 (200 mL·min^{-1}). Each DSC measurement was carried out over three heat-cool cycles. Calculation of percent crystallinity relative to that of elemental sulfur, as reported in Table 1, was done using the equation:

$$\Delta\chi_c = 1 - \left\{ \frac{\Delta H_{m(SPC90)} - \Delta H_{cc\,(SPC90)}}{\Delta H_{m(S)} - \Delta H_{cc(S)}} \right\} \times 100\%$$

where $\Delta\chi_c$ is change of percentage crystallinity with respect to sulfur; $\Delta H_{m(SPC90)}$ is melting enthalpy of composite material **SPC_{90}**; $\Delta H_{cc(SPC90)}$ is cold crystallization enthalpy of composite material **SPC_{90}**; $\Delta H_{m(S)}$ is melting enthalpy of sulfur; $\Delta H_{cc(S)}$ is cold crystallization enthalpy of sulfur

SEM was acquired on a Schottky field emission scanning electron microscope SU5000 operating in variable pressure mode with an accelerating voltage of 15 keV.

Compressional analysis was performed on a Mark-10 ES30 test stand equipped with a M3-200 force gauge (1 kN maximum force with ±1 N resolution) with an applied force rate of 3–4 N·s^{-1}. Compression cylinders were cast from silicone resin molds (Smooth-On Oomoo® 25 tin-cure) with diameters of approximately 6 mm and

heights of approximately 10 mm. Samples were manually sanded to ensure uniform dimensions and measured with a digital caliper with ±0.01 mm resolution. Compressional analysis was performed on at least five samples, and the three most comparable results were averaged.

Flexural strength analysis was performed using a Mettler Toledo DMA 1 STARe System in single cantilever mode. The flexural strength samples were cast from silicone resin molds (Smooth-On Oomoo® 25 tin-cure). The sample dimensions were $1.5 \times 10.4 \times 5.0$ mm. The clamping force was 1 cN m and the temperature was 25 °C. The samples were tested in duplicates, and the results were averaged.

4.2 | Materials, synthesis and fractionation method

Sulfur (Alfa Aesar) and Makrolon™ (Bayer, $M_n = 26{,}400$, $M_w = 57{,}000$, $Đ = 2.2$) were used as received.

> CAUTION: Heating elemental sulfur with organics can result in the formation of H_2S gas. H_2S is toxic, foul-smelling, and corrosive. Although we did not observe any mass loss attributable to gas generation, temperature must be carefully controlled to prevent thermal spikes, contributing to the potential for H_2S evolution. Rapid stirring shortened heating times, and very slow addition of reagents can help prevent unforeseen temperature spikes.

4.3 | Preparation of SPC_{90}

To a Parr bomb reactor were added 13.5 g (0.053 mol) elemental sulfur and 1.50 g (5.90 mmol of repeat unit) PC. The reactor was heated to 320 °C and allowed to run for 2 h before cooling to room temperature. The composite was recovered from the reactor in quantitative yield as a black powder. Elemental analysis calculated: C 7.56, H 0.56, S 90.00; found: C 7.72, H 0.08, S 92.03.

4.4 | Depolymerization of SPC_{90} (d-SPC_{90})

Under an atmosphere of inert N_2 gas, a 100 mg sample of finely ground SPC_{90} and 11 mL dichloromethane were added to a vial, followed by addition of a Teflon-coated magnetic stir bar and 87 mg $AlBr_3$. The vial was sealed with a foil-lined cap and allowed to stir for 30 min at room temperature. The vial was then cooled in an ice bath and a 6 mL aliquot of water was added with stirring. Stirring was stopped and the water layer was removed with a pipet. The water-washing procedure was repeated, and then the organic layer was filtered and volatiles removed by rotary evaporation to yield 40 mg of a tacky, golden brown solid. This solid was the sample used for the IR spectroscopy and GC–MS analysis described in the text.

4.5 | Extraction of dark sulfur

Extraction of dark sulfur was performed recursively by suspending 100.0 mg (weighed on a microbalance) of finely ground material in 20 mL of toluene and stirring the mixture vigorously for 1 h. The solid was then allowing to settle for 30 min and the supernatant was removed via pipet. After drying to constant mass, samples were weighed to determine the masses of the soluble and insoluble fractions. The soluble fraction was found by elemental microanalysis to be >98% sulfur.

ACKNOWLEDGMENTS

This research was funded by the National Science Foundation grant number CHE-2203669. The author primarily responsible for particular CRediT roles are provided here. K. M. Derr: Data curation, Formal analysis, Investigation, Validation, Roles/Writing – original draft. R. C. Smith: Conceptualization, Methodology, Resources, Supervision, Roles/Writing – review and editing.

ORCID

Rhett C. Smith https://orcid.org/0000-0001-6087-8032

REFERENCES

[1] T. Thiounn, M. K. Lauer, M. S. Bedford, R. C. Smith, A. G. Tennyson, *RSC Adv.* **2018**, *8*, 39074.
[2] X. Zhang, Y. Tang, S. Qu, J. Da, Z. Hao, *ACS Catal.* **2015**, *5*, 1053.
[3] A. Demirbas, H. Alidrisi, M. A. Balubaid, *Pet. Sci. Technol.* **2015**, *33*, 93.
[4] G. C. Laredo, J. Reza, E. M. Ruiz, *Cleaner Chem. Eng.* **2023**, *5*, 100094.
[5] Y. Liu, X. B. Lu, *J. Polym. Sci.* **2022**, *60*, 3256.
[6] J. G. Kim, *Polym. Chem.* **2020**, *11*, 4830.
[7] G. W. Coates, Y. D. Getzler, *Nat. Rev. Mater.* **2020**, *5*, 501.
[8] J. M. Payne, M. Kamran, M. G. Davidson, M. D. Jones, *ChemSusChem* **2022**, *15*, e202200255.
[9] V. Martinez Sanz, A. Morales Serrano, M. Schlummer, *Waste Manag. Res.* **2022**, *40*, 1757.
[10] B. Debnath, R. Chowdhury, S. K. Ghosh, In *Urban Min. Sustain. Waste Manag.* Springer, Singapore **2020**, pp. 69-80.

[11] E. Matuszczak, M. D. Komarowska, W. Debek, A. Hermanowicz, *Int. J. Endocrinol.* **2019**, *2019*, 4068717.
[12] J. Zhang, B. Fidalgo, A. Kolios, D. Shen, S. Gu, *Sustain. Energy Fuels* **2017**, *1*, 1788.
[13] J. Zhang, B. Fidalgo, D. Shen, R. Xiao, S. Gu, *J. Anal. Appl. Pyrolysis* **2016**, *122*, 323.
[14] C. Puglisi, L. Sturiale, G. Montaudo, *Macromolecules* **1999**, *32*, 2194.
[15] L.-H. Lee, *J. Polym. Sci. Part A: Gen. Pap.* **1964**, *2*, 2859.
[16] A. Davis, J. Golden, *Die Makromol. Chem.* **2003**, *110*, 180.
[17] A. Davis, J. H. Golden, *Die Makromol. Chem.* **1964**, *78*, 16.
[18] A. Davis, J. H. Golden, *J. Chem. Soc. B: Phys. Org.* **1968**, 40.
[19] K. B. Abbås, *Polymer* **1980**, *21*, 936.
[20] A. C. Hagenaars, W. J. Goddrie, C. Bailly, *Polymer* **2002**, *43*, 5043.
[21] B. N. Jang, C. A. Wilkie, *Thermochim. Acta* **2005**, *426*, 73.
[22] B. N. Jang, C. A. Wilkie, *Polym. Degrad. Stab.* **2004**, *86*, 419.
[23] E. V. Antonakou, D. S. Achilias, *Waste Biomass Valoriz.* **2013**, *4*, 9.
[24] C. Hogue, *Chem. Eng. News* **2022**, *100*, 100.
[25] R. Taurino, P. Pozzi, T. Zanasi, *Waste Manag.* **2010**, *30*, 2601.
[26] C. P. Maladeniya, A. G. Tennyson, R. C. Smith, *J. Polym. Sci.* **2023**, *61*, 787.
[27] G. t. R. C. C. ACI Committee 332, 2006, ACI 332.1R-06, American Concrete Institute, Farmington Hills, MI.
[28] T. Thiounn, M. S. Karunarathna, M. K. Lauer, A. G. Tennyson, R. C. Smith, *RSC Sustain.* **2023**, *1*, 535.
[29] C. V. Lopez, A. D. Smith, R. C. Smith, *Macromol. Chem. Phys.* **2023**, *224*, 2300233. https://doi.org/10.1002/macp.202300233
[30] C. V. Lopez, A. D. Smith, R. C. Smith, *RSC Adv.* **2022**, *12*, 1535.
[31] C. V. Lopez, M. S. Karunarathna, M. K. Lauer, C. P. Maladeniya, T. Thiounn, E. D. Ackley, R. C. Smith, *J. Polym. Sci.* **2020**, *58*, 2259.
[32] J. J. Dale, S. Petcher, T. Hasell, *ACS Appl. Polym. Mater.* **2022**, *4*, 3169.
[33] J. J. Dale, J. Stanley, R. A. Dop, G. Chronowska-Bojczuk, A. J. Fielding, D. R. Neill, T. Hasell, *Eur. Polym. J.* **2023**, *195*, 112198.
[34] J. Bao, K. P. Martin, E. Cho, K.-S. Kang, R. S. Glass, V. Coropceanu, J.-L. Bredas, W. O. N. Parker Jr., J. T. Njardarson, J. Pyun, *J. Am. Chem. Soc.* **2023**, *145*, 12386.
[35] M. S. Karunarathna, A. G. Tennyson, R. C. Smith, *J. Mater. Chem. A* **2020**, *8*, 548.
[36] K. M. Derr, C. V. Lopez, C. P. Maladeniya, A. G. Tennyson, R. C. Smith, *J. Polym. Sci.* **2023**, *5*, 2166.
[37] Y.-S. Lai, Y.-L. Liu, *Macromol. Rapid Commun.* **2023**, *44*, 2300014.
[38] M. S. Karunarathna, M. K. Lauer, A. G. Tennyson, R. C. Smith, *Polym. Chem.* **2020**, *11*, 1621.
[39] W. J. Chung, J. J. Griebel, E. T. Kim, H. Yoon, A. G. Simmonds, H. J. Ji, P. T. Dirlam, R. S. Glass, J. J. Wie, N. A. Nguyen, B. W. Guralnick, J. Park, A. Somogyi, P. Theato, M. E. Mackay, Y.-E. Sung, K. Char, J. Pyun, *Nat. Chem.* **2013**, *5*, 518.
[40] M. S. Karunarathna, M. K. Lauer, T. Thiounn, R. C. Smith, A. G. Tennyson, *J. Mater. Chem. A* **2019**, *7*, 15683.
[41] M. S. Karunarathna, C. P. Maladeniya, M. K. Lauer, A. G. Tennyson, R. C. Smith, *RSC Adv.* **2023**, *13*, 3234.
[42] C. V. Lopez, R. C. Smith, *Mater. Adv.* **2023**, *4*, 2785.
[43] K. A. Tisdale, C. P. Maladeniya, C. V. Lopez, A. G. Tennyson, R. C. Smith, *J. Compos. Sci.* **2023**, *7*, 35.
[44] P. Y. Sauceda-Oloño, A. C. Borbon-Almada, M. Gaxiola, A. D. Smith, A. G. Tennyson, R. C. Smith, *J. Compos. Sci.* **2023**, *7*, 7.
[45] A. Mezencevova, N. N. Yeboah, S. E. Burns, L. F. Kahn, K. E. Kurtis, *J. Environ. Manag.* **2012**, *113*, 128.
[46] S. K. Amin, S. El-Sherbiny, A. A. El-Magd, A. Belal, M. Abadir, *Constr. Build. Mater.* **2017**, *157*, 610.
[47] M. K. Lauer, M. S. Karunarathna, A. G. Tennyson, R. C. Smith, *Mater. Adv.* **2020**, *1*, 590.
[48] M. K. Lauer, M. S. Karunarathna, A. G. Tennyson, R. C. Smith, *Mater. Adv.* **2020**, *1*, 2271.
[49] M. K. Lauer, A. G. Tennyson, R. C. Smith, *Mater. Adv.* **2021**, *2*, 2391.
[50] C. P. Maladeniya, M. S. Karunarathna, M. K. Lauer, C. V. Lopez, T. Thiounn, R. C. Smith, *Mater. Adv.* **2020**, *1*, 1665.
[51] M. K. Lauer, T. A. Estrada-Mendoza, C. D. McMillen, G. Chumanov, A. G. Tennyson, R. C. Smith, *Adv. Sustain. Syst.* **2019**, *3*, 1900062.
[52] M. J. Graham, C. V. Lopez, C. P. Maladeniya, A. G. Tennyson, R. C. Smith, *J. Appl. Polym. Sci.* **2023**, *140*, e53684.

SUPPORTING INFORMATION

Additional supporting information can be found online in the Supporting Information section at the end of this article.

How to cite this article: K. M. Derr, R. C. Smith, *J. Polym. Sci.* **2023**, 1. https://doi.org/10.1002/pol.20230724